AMD-Vol. 145/MD-Vol. 36, Mechanics of Cellulosic Materials
ASME 1992

THE BENDING STIFFNESSES OF CORRUGATED BOARD

S. Luo and J. C. Suhling
Department of Mechanical Engineering
Auburn University
Auburn, Alabama

J. M. Considine and T. L. Laufenberg
U.S.D.A. Forest Products Laboratory
Madison, Wisconsin

ABSTRACT

In this work, an analytical study on the bending stiffnesses of corrugated board has been performed. Formulations to calculate the bending stiffnesses D_{11}, D_{22}, D_{12}, and D_{66} of the equivalent plate representing the corrugated board have been established, and then compared to expressions suggested by other investigators. Several methods for modeling the shape of the corrugated orthotropic medium material have been considered including sinusoidal, arc-and-tangent, and elliptical representations. An extension of the membrane analogy method has been used to calculate the torsional rigidity D_{66} of the corrugated board In addition to the shape of the corrugated core material, the developed stiffness formulations require the thicknesses and material properties of the component paperboards as input.

INTRODUCTION

Unlike fiber-reinforced composite materials, paper (paperboard) is a multiphase composite composed of moisture, fibers, voids, and chemical additives. Its three dimensional structure is basically an assembly of discrete fibers bonded together into a complex network. A single preferred orientation of the fibers results from the hydrodynamic forces present in the papermaking machine. This orientation is called the machine direction (MD). The in-plane direction perpendicular to the preferred direction is called the cross-machine direction (CD). These directions of material symmetry allow for paper to be modeled macroscopically as an orthotropic solid.

The end-use performance characteristics of paperboard products are often predicted using models based upon the measured resistance of the utilized paper materiels to burst, tear, fold, tension, compression, shear, and curl. However, because paperboard is used extensively as a packaging material, the flexural rigidity or bending stiffness of the product is an especially important quantity. In such applications, a stiff paperboard provides the necessary resistance to bulging of the panels of the container, ensuring a high degree of protection for its contents.

Corrugated containers, often referred to erroneously as cardboard boxes, are the most prominent structural application of paper. The corrugated board structural panels comprising such packaging are formed from a pair of flat face plates called liners which are separated by a periodic fluted core referred to as the corrugating medium or medium. Such composite sandwich plates are typically lightweight and inexpensive, and have high stiffness-to-weight and strength-to-weight ratios. Because it is composed of two primary elements, corrugated board is also referred to as combined board. Figure 1 illustrates the basic geometry and component materials of a corrugated board sample. The paper materials used for the liners are usually quite stiff and strong so that the bending stiffness of the combined board is high. The role of the medium material is to maintain separation between the two liners.

New shipping requirements have changed the paperboard market from one based on tonnage to one based on performance. Hence, the structural performance of a corrugated container is the major factor in its success in the marketplace. Such performance is a function of a number of factors including the quality of the input cellulose fibers, the mechanical properties of the utilized linerboard and medium, and the structural properties of the combined board. It is generally agreed that one of the most important attributes of a corrugated board are its bending stiffnesses or flexural rigidities. In order to improve the design and manufacture of corrugated board products, it is necessary to have a clear, technically sound understanding of the contributions of all of these factors to performance.

The primary engineering method for analyzing the mechanical behavior of composite sandwich plate structures such as corrugated board is the use of equivalent plate

models. In such theories, the actual complicated sandwich plate geometry is replaced by an equivalent orthotropic slab of constant thickness having the same or similar bending stiffness characteristics. Subsequent mathematical analyses are then performed using the relatively simple small deflection or large deflection plate theories for orthotropic materials. This conceptual substitution of a single sheet of uniform material for the true composite structural panel is by its nature an approximation. However, the equivalent plate technique has proved to be a useful, expedient, and accurate method for predicting the transverse deformations of stiffened plates such as corrugated board. The utility of the equivalent plate method can be appreciated further by considering the available alternatives. These include trial and error procedures which lack predictive qualities, and costly time-consuming three-dimensional finite element analyses.

Equivalent plate models have been used for a variety of stiffened structures including ribbed plates, plate girders, reinforced or prestressed elements, and composite beam gridworks. Such composite structural elements are often referred to as being "technically orthotropic" since they are modeled as a single orthotropic layer. Several extensive reviews of the published applications of equivalent plate models are available in the literature. These include the works of Troitsky [1,2], and Bares and Massonnet [3].

Prior investigations on particular stiffened plate configurations have adopted either analytical or experimental strategies to obtain the required bending stiffnesses. In the theoretical approach, analytical expressions are developed to predict the equivalent orthotropic bending stiffnesses of the stiffened plate. Input parameters to these formulas typically include the mechanical properties of the component materials and relevant geometrical dimensions and characteristics. In the experimental approach, measurements of the force versus deflection response of the actual stiffened plate are used to establish the equivalent flexural rigidities. The stiffnesses found using either procedure are then typically used as input to the governing equation of the classical small deflection orthotropic plate theory. This equation for the transverse deflection of the plate can be solved by a variety of relatively straight-forward techniques including analytical closed-form solution procedures and the finite element method.

Equivalent plate models for corrugated sheets formed from isotropic materials and without face plates have been considered by several investigators. Seydel [4] presented a set of formulas for predicting the bending stiffnesses of a sinusoidal corrugated sheet. He then applied the results to predict shear buckling behavior. The same theoretical equations for sinusoidal corrugations were later presented by Lekhnitskii [5], Szilard [6], and Troitsky [1].

The flexural rigidities of isotropic panels with a periodic corrugation made of straight line segments were measured experimentally by Kinloch and Harvey [7]. The shape of the corrugation in their investigation was nearly a square wave. Essentially the same corrugation pattern had been studied earlier by Libove and Hubka [8] using analytical methods. In their work, twin face plates were used to sandwich the corrugated core sheet. Also, a higher order shear plate theory was considered

Expressions for the moment of inertia per unit length of single sheets with arc-and-tangent type corrugation have been given by Blodgett [9] and Wolford [10]. This type of corrugation pattern is formed using circular arcs and straight lines, and is often used for roofing, siding, and drainage conduits. The straight lines connect to the circular arcs along the tangent lines to the arcs, so that the slopes of the corrugation are continuous.

There have numerous investigations on the bending stiffnesses of the corrugated board used by the paper industry. The majority of these studies have considered either theories or experiments to find one or more of flexural rigidities of the board. Since a plate theory analysis was not considered in many of the investigations, the bending stiffnesses were often defined using formulas appropriate for beams instead of plates. In the beam approach, the bending stiffness is defined as the product of an elastic modulus term with a moment of inertia term ($D = EI$). For plates, the bending stiffnesses typically have the form of the beam bending stiffness multiplied by a Poisson's ratio interaction term which characterizes the two-dimensional nature of the plate ($D = EIf(\nu)$). The use of beam-like bending stiffnesses to characterize corrugated board has been widely propagated by the popularity of the so-called McKee formula [11-12] for the compression strength of a corrugated box. This well-known equation requires two beam bending stiffnesses of the corrugated board as input. These are typically evaluated experimentally by performing four point bending tests on corrugated board strips (which behave as beams).

In the early theoretical studies of Kellicutt and Peters [13], and Kellicutt [14], formulas were derived to calculate the moments of inertia of the liners and medium comprising corrugated board. These expressions were then used to calculate the beam bending stiffnesses ($D = EI$) of several kinds of corrugated board. The shape of the fluted medium in these investigations was assumed to be semi-elliptical.

An improved methodology for calculating the contributions to the bending stiffnesses of corrugated board beams ($D = EI$) due to the medium was later suggested by Banger [15] and Peterson [16]. In these separate but identical studies, the shape of the corrugated medium was modeled in a more representative manner using a periodic sine function. The cross-sectional area of the medium was assumed to have constant thickness measured perpendicular to its sinusoidal middle surface. A numerical procedure was suggested to calculate the moment of inertia of this area. This method requires that the thin sinusoidal cross-sectional area of the medium be divided up into a large number of short segments which are nearly rectangular. The total moment of inertia is then found by summing up the contributions of these small area elements.

Relatively simple closed-form expressions for the bending stiffnesses of corrugated board beams ($D = EI$) were suggested by Carlsson, Fellers, and Jonsson [17]. In their work, the shape of the middle surface of the cross-sectional area of the corrugated medium was again represented using a periodic harmonic function. However, the thickness of the curved medium was allowed to vary slightly so that a pair of cosine functions could be used to completely describe the outside border of its cross-sectional area With these approximations, a relatively simple formula for the moment of inertia per unit length of the medium was found.

Pommier, et al. [18] later used this moment of inertia formula in a set of expressions they proposed for the four plate bending stiffnesses of corrugated board ($D = EIf(v)$). Their formulations were based upon extending the bending stiffness equations appropriate for a single layer orthotropic plate. These authors have also used the finite element method to calculate the equivalent plate bending stiffnesses of corrugated board sheets [19]. In that work the corrugated sheet was itself treated like an engineering structure, and the liners and medium were meshed with plate elements. The medium was modeled as a set of trapezoidal flutings, similar to the model used by Urbanik [20]. The equivalent plate bending stiffnesses of the corrugated board sheet were then calculated by using the finite element predictions for loading geometries where there are known analytical solutions for analogously loaded single layer orthotropic plates.

The orthotropic version of the von Karman large deflection plate theory has been applied to an equivalent plate representation of corrugated board by Peterson and Fox [21], and Peterson [22]. In these investigations, the Rayleigh-Ritz method was employed to predict approximate displacement and stress fields in rectangular corrugated board panels subjected to simple loadings. The required plate bending stiffnesses were approximated using extensions of the bending stiffness formulas for a single-layer orthotropic plate, and the moment of inertia of the medium was calculated using the method presented by Peterson [16].

The investigations by Pommier, et al. [19-20], and Peterson, et al. [21-22] appear to be the only cases where correct differentiations between the beam and plate bending stiffnesses of corrugated board have been made. In this work, an analytical study on the plate bending stiffnesses of corrugated board has been performed. Formulations to calculate the bending stiffnesses D_{11}, D_{22}, D_{12}, and D_{66} of the equivalent plate representing the corrugated board have been established, and then compared to expressions suggested by other investigators. Several methods for modeling the shape of the corrugated orthotropic medium material have been considered including sinusoidal, arc-and-tangent, and elliptical representations. An extension of the membrane analogy method has been used to calculate the torsional rigidity D_{66} of the corrugated board. In addition to the shape of the corrugated core material, the developed stiffness formulations require the thicknesses and material properties of the component paperboards as input.

THEORETICAL PRELIMINARIES

Orthotropic Stress-Strain Relations

A thin orthotropic plate is shown in Figure 2. The coordinate axes have been chosen so that they are aligned with the material symmetry directions of the material, and so that the x-y plane is the middle surface of the plate. If the material is linear elastic and in a state of plane stress, the stress-strain relations are [1-3,5-6]

$$\begin{aligned} \epsilon_x &= S_{11}\sigma_x + S_{12}\sigma_y \\ \epsilon_y &= S_{12}\sigma_x + S_{22}\sigma_y \\ \gamma_{xy} &= S_{66}\tau_{xy} \end{aligned} \tag{1}$$

The material compliances S_{ij} are defined by

$$\begin{aligned} S_{11} &= \frac{1}{E_1} \\ S_{12} &= -\frac{\nu_{12}}{E_1} = -\frac{\nu_{21}}{E_2} \\ S_{22} &= \frac{1}{E_2} \\ S_{66} &= \frac{1}{G_{12}} \end{aligned} \tag{2}$$

where E_1 and E_2 are the elastic moduli, ν_{12} and ν_{21} are the Poisson's ratios, and G_{12} is the shear modulus. Equation (1) can be inverted to give

$$\begin{aligned} \sigma_x &= Q_{11}\epsilon_x + Q_{12}\epsilon_y \\ \sigma_y &= Q_{12}\epsilon_x + Q_{22}\epsilon_y \\ \tau_{xy} &= Q_{66}\gamma_{xy} \end{aligned} \tag{3}$$

where the so-called reduced stiffnesses Q_{ij} are given by

$$\begin{aligned} Q_{11} &= \frac{E_1}{1 - \nu_{12}\nu_{21}} \\ Q_{12} &= \frac{\nu_{12}E_2}{1 - \nu_{12}\nu_{21}} = \frac{\nu_{21}E_1}{1 - \nu_{12}\nu_{21}} \\ Q_{22} &= \frac{E_2}{1 - \nu_{12}\nu_{21}} \\ Q_{66} &= G_{12} \end{aligned} \tag{4}$$

Orthotropic Plate Theory

The classical small deflection theory for linear elastic orthotropic plates is a formulation describing the behavior of thin plates subjected to transverse loading. The transverse deflections of the plate are assumed to be small relative to its thickness. The governing equation for the transverse deflection is given by [1-3,5-6]

$$D_{11}\frac{\partial^4 w}{\partial x^4} + 2(D_{12} + 2D_{66})\frac{\partial^4 w}{\partial x^2 \partial y^2} + D_{22}\frac{\partial^4 w}{\partial y^4} = p(x,y) \tag{5}$$

where $w = w(x,y)$ is the transverse deflection of the middle surface of the plate, h is the plate thickness, $p(x,y)$ is the transverse pressure loading on the plate, and

$$D_{11} = \frac{h^3}{12}Q_{11} = \frac{E_1h^3}{12(1 - \nu_{12}\nu_{21})}$$

$$D_{22} = \frac{h^3}{12}Q_{22} = \frac{E_2h^3}{12(1 - \nu_{12}\nu_{21})}$$

$$D_{12} = \frac{h^3}{12}Q_{12} = \frac{\nu_{21}E_1h^3}{12(1 - \nu_{12}\nu_{21})} = \frac{\nu_{12}E_2h^3}{12(1 - \nu_{12}\nu_{21})} \tag{6}$$

$$D_{66} = \frac{h^3}{12}Q_{66} = \frac{G_{12}h^3}{12}$$

are the bending stiffnesses or flexural rigidities of the anisotropic plate. The term

$$H = D_{12} + 2D_{66} \tag{7}$$

is often called the total torsional rigidity. The stiffness D_{66} is often referred to as the apparent torsional rigidity or simply the torsional rigidity.

The in-plane stresses for a plate subjected to transverse loading are given by

$$\sigma_x = \frac{12M_x}{h^3}z$$

$$\sigma_y = \frac{12M_y}{h^3}z \tag{8}$$

$$\tau_{xy} = \frac{12M_{xy}}{h^3}z$$

where the bending moment resultants (bending moments per unit length) are defined as

$$M_x = -\left[D_{11}\frac{\partial^2 w}{\partial x^2} + D_{12}\frac{\partial^2 w}{\partial y^2}\right]$$

$$M_y = -\left[D_{12}\frac{\partial^2 w}{\partial x^2} + D_{22}\frac{\partial^2 w}{\partial y^2}\right] \tag{9}$$

$$M_{xy} = -2D_{66}\frac{\partial^2 w}{\partial x \partial y}$$

Equivalent Plate Models

The idea of applying the classical theory of orthotropic plates to slabs stiffened by ribs was proposed and developed by Huber [23]. The basic assumption he proposed for estimating bending deflections in a stiffened slab, was to replace such a slab by an equivalent orthotropic plate of constant thickness having the same stiffness characteristics. Since corrugated boards are composed of two liners and one medium, the idea of an equivalent plate having the same stiffness characteristics can be introduced However, it should be understood that the actual corrugated board obviously can't be modeled accurately by the equivalent plate in every respect.

Former theoretical investigations and experimental data have indicated that the equivalent plate concept is applicable to more complicated stiffened/sandwich plates such as corrugated board under the following provisions [1]:

1. The ratios of the periodic length of the medium to the plate boundary dimensions are small enough to insure approximate homogeneity of the stiffnesses.
2. The rigidities are uniformly distributed in both directions.
3. The flexural and twisting rigidities do not depend on the boundary conditions of the plate or on the distribution of the vertical load.
4. A perfect bond exists between the liners and the medium.

The substitution of an equivalent plate with the same stiffness characteristics as corrugated board has been called the method of elastic equivalence. By applying the principle of elastic equivalence, the discontinuous structure of the corrugated sandwich plate is represented by an idealized constant thickness orthotropic plate, which reflects the stiffnesses of the actual system. This substitution is illustrated in Figure 3. When using the equivalent plate method, structural orthotropy is replaced by natural orthotropy, and eq. (5) is used as the governing differential equation for the out-of plane displacements of the corrugated plate. It should be noted, however, that stress distributions in the corrugated board cannot be found using eqs. (8) because of the discontinuous nature of the corrugated board structure when compared to its equivalent plate representation.

A common way to estimate the appropriate bending stiffnesses to use in eq. (5) for complicated stiffened/sandwich plates is to consider a simple extension of the relations for single layer orthotropic plates in eq. (6). These expressions can be recast in the form

$$D_{11} = \frac{E_1 I}{1 - \nu_{12}\nu_{21}}$$

$$D_{22} = \frac{E_2 I}{1 - \nu_{12}\nu_{21}} \tag{10}$$

$$D_{12} = \nu_{21}D_{11} = \nu_{12}D_{22}$$

$$D_{66} = G_{12}I$$

where

$$I = I_{xx} = I_{yy} = \frac{h^3}{12} \tag{11}$$

is the area moment of inertia per unit length about the x and y axes for the cross-sectional areas of the plate which are normal to the y and x axes, respectively. Since these two moments of inertia are typically different for a stiffened/sandwich plate, the first two expressions in eqs. (10) are typically generalized to [1-3]

$$D_{11} = \frac{E_1 I_{yy}}{1 - \nu_{12}\nu_{21}}$$
$$D_{22} = \frac{E_2 I_{xx}}{1 - \nu_{12}\nu_{21}} \tag{12}$$

There is no clear way to generalize the last two expressions in eqs. (10). The presence of unequal moments of inertia will lead to discrepancies in the two expressions for D_{12} since it is likely that

(13)

Also, it is not clear which of the two moments of inertia to use in the expression for D_{66}.

ANALYTICAL STIFFNESS CALCULATIONS FOR CORRUGATED BOARD

Initial Assumptions

The characteristic geometry and dimensions of corrugated board are shown in Figure 4. In this illustration, h is the thickness of the liners, t is the thickness of the medium, L is one half of the wave length of the periodic fluting, and H is one half of the flute height (the distance from the middle surface of the board to the middle surface of the medium at its extreme positions). As indicated previously in Figure 1, the x and y directions are chosen along and perpendicular to the fluting "propagation" direction.

Since the geometry of corrugated board is so complicated, several intuitive assumptions need to be made to simplify the modeling procedure and establish tractable formulations for the stiffnesses. First, it is assumed that a superposition principle exists where the flexural rigidities of liners and medium can be added together to yield the total stiffnesses. The stiffnesses then are given by

$$\begin{aligned} D_{11} &= D^l_{11} + D^m_{11} \\ D_{22} &= D^l_{22} + D^m_{22} \\ D_{12} &= D^l_{12} + D^m_{12} \\ D_{66} &= D^l_{66} + D^m_{66} \end{aligned} \tag{14}$$

The superscripts 1 and m in eq. (14) refer to the liner and medium papers, respectively. Second, it is assumed that generalizations in eq. (12) can be applied individually to both the liners and the medium. Therefore, the stiffnesses D_{11} and D_{22} for the individual components of the combined board are given by

$$D^l_{11} = \frac{E^l_1}{1 - \nu^l_{12}\nu^l_{21}} I^l_{yy} \qquad D^l_{22} = \frac{E^l_2}{1 - \nu^l_{12}\nu^l_{21}} I^l_{xx} \tag{15}$$

$$D^m_{11} = \frac{E^m_1}{1 - \nu^m_{12}\nu^m_{21}} I^m_{yy} \qquad D^m_{22} = \frac{E^m_2}{1 - \nu^m_{12}\nu^m_{21}} I^m_{xx} \tag{16}$$

The quantities I^1_{xx} and I^1_{yy} in eq. (15) are the moments of inertia per unit length of the liner about the x and y axes, respectively. Similarly, the quantities I^m_{xx} and I^m_{yy} in eq. (15) are the momenta of inertia per unit length of the medium about the x and y axes, respectively. Combining eqs. (14-16), The expressions for D_{11} and D_{22} of corrugated board can be written as

$$\begin{aligned} D_{11} &= \frac{E^l_1}{1 - \nu^l_{12}\nu^l_{21}} I^l_{yy} + \frac{E^m_1}{1 - \nu^m_{12}\nu^m_{21}} I^m_{yy} \\ D_{22} &= \frac{E^l_2}{1 - \nu^l_{12}\nu^l_{21}} I^l_{xx} + \frac{E^m_2}{1 - \nu^m_{12}\nu^m_{21}} I^m_{xx} \end{aligned} \tag{17}$$

Calculation of D_{11} and D_{22} for the Liners

Referring to Figures 4 and 5, the liner moments of inertia per unit length I^1_{xx} and I^1_{yy} are equal to each other and given by

$$\begin{aligned} I^l_{xx} = I^l_{yy} &= 2\int_{H+\frac{t}{2}}^{H+\frac{t}{2}+h} z^2\,dz \\ &= 2\left(H + \frac{t}{2}\right)^2 h + 2\left(H + \frac{t}{2}\right)h^2 + \frac{2h^3}{3} \end{aligned} \tag{18}$$

Substituting eq. (18) into eqs. (15), the flexural rigidities of the liners then become

$$\begin{aligned} D^l_{11} &= \frac{E^l_1}{1 - \nu^l_{12}\nu^l_{21}}\left[2\left(H + \frac{t}{2}\right)^2 h + 2\left(H + \frac{t}{2}\right)h^2 + \frac{2h^3}{3}\right] \\ D^l_{22} &= \frac{E^l_2}{1 - \nu^l_{12}\nu^l_{21}}\left[2\left(H + \frac{t}{2}\right)^2 h + 2\left(H + \frac{t}{2}\right)h^2 + \frac{2h^3}{3}\right] \end{aligned} \tag{19}$$

Plate bending stiffness expressions for the liners which are equivalent to those in eq. (19) have been presented previously by Pommier, et al. [18] and Peterson, et al, [21-22].

Calculation of D_{11} and D_{22} for the Corrugated Medium

As shown in Figure 6, the medium has corrugations along the x- direction which is also its machine direction. The thickness of the medium paper is usually very small. Also, the moment of inertia I^m_{yy} takes on several values (including approximately zero when the medium cross-sectional area is at z = 0) as different cross-sections are considered along the x-azis. In this work, as in references [18, 21-22], the conservative assumption

$$I^m_{yy} \approx 0 \tag{20}$$

has been adopted Therefore, from eq. (16)

$$D^m_{11} = 0 \tag{21}$$

To calculate the moment of inertia I^m_{xx}, the shape and configuration of the corrugated medium material must be

assumed. Once the moment of inertia is calculated, the flexural rigidity of the corrugated medium can be approximated using the second of eqs. (16). Referring to Figure 7, the moment of inertia of the corrugated medium per unit length can be calculated using

$$I_{xx}^{m} = \frac{1}{L}\int_0^L \int_{f_b(x)}^{f_t(x)} z^2 dz\, dx \tag{22}$$

The functions $f_t(x)$ and $f_b(x)$ represent the top and bottom boundary curves of the medium, respectively. The desired moment of inertia is then the area moment of inertia of the area A_m between these lines, as shown in Figure 8. It is often not easy to calculate the moment of inertia of this area. The moment of inertia of the shaded area A'_m shown in Figure 9 is more easily calculated in some cases. This is done by subtracting the moment of inertia I, of the shaded area A_t under the top curve from the moment of inertia I, of the shaded area A_b under the bottom curve, as shown in Figure 10. Referring to Figure 11, the only difference between the moments of inertia of the areas in Figures 8 and 9 is to calculate the moment of inertia of the small triangular area A, instead of A_2. Since these two areas are very small and close to the x-axis, it is accurate enough to calculate the moment of inertia I_{xx}^{m} using the area in Figure 9 and the equation

$$I_{xx}^{m} = \frac{I_t - I_b}{L} \tag{23}$$

where I, and I, are the moments of inertia of areas A_t and A_b shown in Figure 10.

In order to calculate the moment of inertia I_{xx}^{m} using either eq. (22) or eq. (23), the function $f_c(x)$ describing the middle surface of the corrugated medium must be assumed There are several possible ways to represent this function. In the past, it has been assumed to be elliptical [13], sinusoidal [15-18,21-22] and composed of circular arcs and straight lines (arc-and-tangent shape) [24]. Several methods to calculate I_{xx}^{m} are now presented and then compared.

[a] Sinusoidal Medium - Constant Thickness

In this method, the middle surface is assumed as sine curve, i.e.

$$f_c(x) = H\sin\frac{\pi x}{L} \tag{24}$$

Since the thickness of the medium is considered to be constant, functions $f_t(x)$ and $f_b(x)$ are then separated from $f_c(x)$ by a perpendicular distance of t/2. This is shown graphically using points P, Q, and S in Figure 12. Using vector methods and appropriate changes of variables, it is possible to express the integrals I_t and I_b for the moments of inertia of areas A_t and A_b (see Figure 10) as [25]

$$\begin{aligned} I_t &= \frac{2}{3}\int_{x_t}^{\frac{L}{2}} (F_1 + F_2)^3 \left[1 + \frac{F_3 - F_4}{F_5}\right] dx \\ I_b &= \frac{2}{3}\int_{x_b}^{\frac{L}{2}} (F_1 - F_2)^3 \left[1 - \frac{F_3 - F_4}{F_5}\right] dx \end{aligned} \tag{25}$$

where functions F_i are defined by

$$\begin{aligned} F_1(x) &= f_c(x) = H\sin\frac{\pi x}{L} \\ F_2(x) &= \frac{t}{2\sqrt{1 + \frac{H^2\pi^2}{L^2}\cos^2\frac{\pi x}{L}}} \\ F_3(x) &= \frac{Ht\pi^2}{L^2}\sqrt{1 + \frac{H^2\pi^2}{L^2}\cos^2\frac{\pi x}{L}}\ \sin\frac{\pi x}{L} \\ F_4(x) &= \frac{tH^3\pi^4}{L^4}\left[1 + \frac{H^2\pi^2}{L^2}\cos^2\frac{\pi x}{L}\right]^{-\frac{1}{2}}\cos^2\frac{\pi x}{L}\sin\frac{\pi x}{L} \\ F_5(x) &= 2\left[1 + \frac{H^2\pi^2}{L^2}\cos^2\frac{\pi x}{L}\right] \end{aligned} \tag{26}$$

and where

$$\begin{bmatrix} x_t \\ x_b \end{bmatrix} = \pm\frac{1}{2\pi}\cos^{-1}\left(\frac{-1 + \sqrt{1 + \frac{\pi^2}{L^2}\left(2H^2 + \frac{H^4\pi^2}{L^2} - t^2\right)}}{\frac{H^2\pi^2}{L^2}}\right) \tag{27}$$

are the x-intercepts of the functions $f_t(x)$ and $f_b(x)$, as shown in Figure 12.

Once the integrals in eqs. (25) are evaluated, the moment of inertia of the medium per unit length, I_{xx}^{m}, is obtained by using eq. (23). Although the integrals in eqs. (25) are difficult, they can be routinely evaluated using numerical integration procedures.

[b] Sinusoidal Corrugation - Approximate Method

Since the constant thickness calculation in the last section is so complicated, an approximate method has been developed where two different sine functions are used to represent the top and bottom curves. This technique is very similar to the procedure implemented by Carlsson, et al. [17] using cosine functions. Referring to Figure 13, the function for the sinusoidal middle line of the medium is again given by eq. (24). The slope of this curve at the origin is

$$f_c'(0) = \frac{H\pi}{L} = \tan\theta \tag{28}$$

so that

$$\theta = \tan^{-1}\left[\frac{H\pi}{L}\right] \tag{29}$$

If the medium thickness is taken as t at the origin, the distance $\overline{oa}$ is t/2. Using trigonometry, the distance $\overline{ob}$ is

$$\overline{ob} = \frac{t}{2}\csc\theta = \frac{t\sqrt{H^2\pi^2 + L^2}}{2\pi H} = \overline{ob'} \tag{30}$$

The functions representing the top and bottom curves are zero at points b and b', respectively. Also, the amplitude of the top curve is (H + t/2) at x = L/2 and the amplitude of the bottom curve is (H - t/2) at x = L/2. The two sine functions which satisfy these x-intercept and amplitude conditions are

$$f_t(x) = (H + \frac{t}{2})\sin\frac{\pi\left[x + \frac{t}{2\pi H}\sqrt{H^2\pi^2 + L^2}\right]}{\left[L + \frac{t}{\pi H}\sqrt{H^2\pi^2 + L^2}\right]} \tag{31}$$

$$f_b(x) = (H - \frac{t}{2})\sin\frac{\pi\left[x - \frac{t}{2\pi H}\sqrt{H^2\pi^2 + L^2}\right]}{\left[L - \frac{t}{\pi H}\sqrt{H^2\pi^2 + L^2}\right]} \tag{32}$$

Using eqs. (31,32) to set up integrals for the moments of inertia I_t and I_b, and then substituting the calculated results into eq. (23) gives

$$I_{xx}^m = \frac{4}{3\pi}\left[H^2t + \frac{t^3}{12}\right] + \frac{2}{9\pi^2 L}(4H^2t + 3Ht^3)\sqrt{\pi^2 + \frac{L^2}{H^2}} \tag{33}$$

Equation (33) is an approximate formula for a sinusoidal corrugation shape which can be easily calculated by hand

[c] Semi-Elliptical Corrugation Shape

Kellicutt and Peters [13] have presented a moment of inertia formula which is based on the assumption that the shape of the medium is semi-elliptical, as shown in Figure 14. The formula for calculating the moment of inertia per unit length of the corrugated medium is

$$I_{xx}^m = \frac{\pi(a^3c - a_1^3c_1)}{8L} \tag{34}$$

where the characteristic dimensions of the ellipse a, a_1, c, c_1 are defined in Figure 14. By comparing Figure 14 to Figure 13, these distances can be related to H, L, and t:

$$a = H + \frac{t}{2} \qquad a_1 = H - \frac{t}{2}$$
$$c = \frac{1}{2}(L + t) \qquad c_1 = \frac{1}{2}(L - t) \tag{35}$$

Substitution of eq. (35) into eq. (34) yields

$$I_{xx}^m = \frac{\pi}{16L}\left[\left(H + \frac{t}{2}\right)^3(L + t) - \left(H - \frac{t}{2}\right)^3(L - t)\right] \tag{36}$$

[d] Arc-and-tangent Corrugation Shape

Blodgett [9] and Wolford [10] have calculated the moment of inertia per unit length of a corrugated plate with arc-and-tangent type corrugation as shown in Figure 15. In addition to the dimensions H, L, and t used for other corrugating shapes, the arc-and-tangent form has three additional geometric parameters m, α, and r. Only four of these six parameters are unique. Trigonometry can be used to obtain the dependence relations

$$r = \frac{\frac{L}{2}\sin\alpha - H\cos\alpha}{1 - \cos\alpha} \tag{37}$$
$$m = 2H(\csc\alpha + \cot\alpha) - L$$

The moment of inertia per unit length is obtained by combining of the moments of inertia of the tangent line and the arc

$$I_{xx}^m = \frac{I_L + I_A}{L} \tag{38}$$

where I_L is the moment of inertia of the straight tangent line with respect to x-axis, and I_A is the moment of inertia of the circular arc with respect to the x-axis.

The moment of inertia of the straight line, I_L, can be calculated using the integral

$$I_L = \int_{-\frac{m}{2}}^{\frac{m}{2}}\int_{-\frac{t}{2}}^{\frac{t}{2}}(S^2\sin^2\alpha + T^2\cos^2\alpha + 2ST\sin\alpha\cos\alpha)\,dS\,dT$$
$$= \frac{m^3t}{12}\sin^2\alpha + \frac{mt^3}{12}\cos^3\alpha \tag{39}$$

where S and T are a set of cartesian coordinate axes rotated by an angle α from the x and z axes.

The moment of inertia of the arc with respect to the x-axis is equal to the moment of inertia of the arc with respect to a parallel axis through the center of the circle added to appropriate parallel axis theorem terms. Performing this calculation gives

$$I_A = \frac{1}{2}(4r^3t + rt^3)(\frac{\alpha}{2} + \frac{\sin 2\alpha}{4}) + 2rt\alpha(H - r)^2$$
$$+ (H - r)(4r^2t + \frac{t^3}{3})\sin\alpha \tag{40}$$

Substituting eqs. (39,40) into eq. (38) yields the desired moment of inertia per unit length

$$I_{xx}^{m} = \frac{1}{24L}[r(6\alpha + 3\sin 2\alpha - 8\sin\alpha) + 8H\sin\alpha + 2m\cos^2\alpha]t^3$$

$$+ \frac{1}{2L}[r^3(6\alpha + \sin 2\alpha - 8\sin\alpha) + 8Hr^2(\sin\alpha - \alpha) \qquad (41)$$

$$+ 4H^2\alpha r + \frac{m^3}{6}\sin^2\alpha]t$$

In this work, the shape of the arc-and-tangent curve was specified using four parameters which were the length L, height H, thickness t, and angle α. Parameters m and r could then be easily found using eqs. (37). The values for L, H, and t of a medium are usually specified regardless of the assumed shape of the periodic fluting. In order to get the value of a, a trial and error method was used. This procedure attempted to find the closest match of the arc-and-tangent shape to a sinusoidal middle surface.

[e] Ranger-Peterson Method

Banger [15] and Peterson [16] have presented a method for calculating the moment of inertia for the corrugated medium which relies upon summing the moments of inertia of a set of rectangular areas making up the medium's cross-sectional area. Referring to Figure 16, the moment of inertia of an arbitrary rectangular segment is

$$I_i = \iint Z^2 dA + Az_0^2 \qquad (42)$$

where

$$A = st \qquad (43)$$

is the area of the rectangle, and Z is the distance from dA to the X-axis. The (X,Z) and (S,T) coordinates are related by the transformation

$$\begin{bmatrix} X \\ Z \end{bmatrix} = \begin{bmatrix} \cos\theta & -\sin\theta \\ \sin\theta & \cos\theta \end{bmatrix} \begin{bmatrix} S \\ T \end{bmatrix} \qquad (44)$$

Using eq. (44), the integral in eq. (42) can be rewritten as

$$I_i = \int_{-s/2}^{s/2}\int_{-t/2}^{t/2} (S^2\sin^2\theta + T^2\cos^2\theta + 2ST\cos\theta\sin\theta + z_0^2)|J|dSdT \qquad (45)$$

where

$$|J| = \text{Jacobian} = \det\begin{bmatrix} \cos\theta & -\sin\theta \\ \sin\theta & \cos\theta \end{bmatrix} = 1 \qquad (46)$$

Evaluating the integral in eq. (45) gives

$$I_i = \frac{s^3t}{12}\sin^2\theta + \frac{st^3}{12}\cos^2\theta + z_0^2 st \qquad (47)$$

The total moment of inertia of the medium per unit length can be found by adding up the contributions from a set of N rectangles which comprises the medium's cross-sectional area

$$I_{xx}^{m} = \frac{\sum_i^N I_i}{L} \qquad (48)$$

In this work, eq. (48) was evaluated numerically using eq. (47) and a sinusoidal middle surface corrugation shape.

Comparison of the Methods for I_{xx}^{m}

Three corrugation shapes referred to as A, B, and C flute, have been used as examples to compare the various methods of modeling the medium which were discussed in the last several sections. Typical characteristic dimensions for these flute sizes are given in Figure 17. The results for I_{xx}^{m} using the various methods applied to the three flute sizes are shown in Figure 18. All but those of the semi-elliptical method match very closely. This suggests that the sinusoidal corrugation approximate method (I_{xx}^{m} from eq. (33)) provides the best compromise between speed and accuracy.

Calculation of D_{11} of D_{22} for the Combined Board

Using eqs. (14-17,19,21), final expressions can now be presented for the stiffnesses D_{11} and D_{22} of corrugated board:

$$D_{11} = \frac{E_1^l}{1 - \nu_{12}^l\nu_{21}^l}\left[2\left(H + \frac{t}{2}\right)^2 h + 2\left(H + \frac{t}{2}\right)h^2 + \frac{2h^3}{3}\right]$$

$$D_{22} = \frac{E_2^l}{1 - \nu_{12}^l\nu_{21}^l}\left[2\left(H + \frac{t}{2}\right)^2 h + 2\left(H + \frac{t}{2}\right)h^2 + \frac{2h^3}{3}\right] \qquad (49)$$

$$+ \frac{E_2^m}{1 - \nu_{12}^m\nu_{21}^m} I_{xx}^m$$

Several possible formulas for the moment of inertia I_{xx}^{m} have be given in the previous sections (see eqs. (25-27,33,36,41,48)).

Calculation of D_{12}

The formula for D_{12} of a single layer orthotropic plate was shown in eq. (10). As presented earlier in eq. (14), it is assumed that the total stiffness of corrugated board can be expressed as a sum of contributions from the liner and medium

$$D_{12} = D_{12}^l + D_{12}^m \qquad (50)$$

The liner and medium stiffnesses needed in eq. (50) can be approximated by extending the single layer plate results in eq. (10)

$$D_{12}^l = \nu_{12}^l D_{22}^l \quad \text{or} \quad D_{12}^l = \nu_{21}^l D_{11}^l$$

$$D_{12}^m = \nu_{12}^m D_{22}^m \quad \text{or} \quad D_{12}^m = \nu_{21}^m D_{11}^m \qquad (51)$$

Using eqs. (19) and the relationship $\nu_{12}E_2 = \nu_{21}E_1$ between the properties of an orthotropic material, it can be easily established that both expressions for D_{12}^l give the same result

$$D_{12}^l = \nu_{12}^l D_{22}^l = \nu_{21}^l D_{11}^l \qquad (52)$$

However, the two expressions for D_{12}^m give contradictory

results since the moments of inertia I^m_{xx} and I^m_{yy} are not equal. To avoid such contradictions, it is suggested that the D^m_{12} expressions in eq. (51) be modified to weight the two possibilities equally. This yields

$$D^m_{12} = \frac{1}{2}[\nu^m_{12} D^m_{22} + \nu^m_{21} D^m_{11}] \approx \frac{1}{2}\nu^m_{12} D^m_{22} \qquad (53)$$

where eq. (21) has been used to simplify the expression. Substitution of eqs. (52,53) into eq. (50) gives the final expression for D_{12}

$$\begin{aligned} D_{12} &= \nu^l_{12} D^l_{22} + \frac{1}{2}\nu^m_{12} D^m_{22} \\ &= \nu^l_{21} D^l_{11} + \frac{1}{2}\nu^m_{12} D^m_{22} \end{aligned} \qquad (54)$$

In references [18,21-22], it has been suggested to neglect the contribution of the medium in eq. (54).

Torsional Rigidity D_{66}

The formula for D_{66} of a single layer orthotropic plate was shown in eq. (10). As presented earlier in eq. (14), it is assumed that the total stiffness of corrugated board can be expressed as a sum of contributions from the liner and medium

$$D_{66} = D^l_{66} + D^m_{66} \qquad (55)$$

The liner and medium stiffnesses needed in eq. (55) can be approximated by extending the single layer plate results in eq. (10)

$$\begin{aligned} D^l_{66} &= G^l_{12} I^l_{xx} \quad \text{or} \quad D^l_{66} = G^l_{12} I^l_{yy} \\ D^m_{66} &= G^m_{12} I^m_{xx} \quad \text{or} \quad D^m_{66} = G^m_{12} I^m_{yy} \end{aligned} \qquad (56)$$

Arguments similar to those made in the last section for D_{12} can now be made. Again, it is suggested that to avoid contradictions, the expressions in eq. (56) for the medium be modified to weight the two possibilities equally. Using eqs. (19,21), this leads to:

$$\begin{aligned} D_{66} &= G^l_{12} I^l_{xx} + \frac{1}{2} G^m_{12} I^m_{xx} \\ &= G^l_{12} I^l_{yy} + \frac{1}{2} G^m_{12} I^m_{xx} \end{aligned} \qquad (57)$$

In reference [18], it has been suggested to modify eq. (57) to include twice the contribution of the medium. In references [21-22], it has been suggested to neglect the contribution of the medium in eq. (57).

Bares and Massonnet [3] have developed a alternative method to calculate the torsional rigidity of an open slab stiffened with beams, and of hollow box sections with upper and lower plates of equal thickness. In this method, the theory of torsion and the method of membrane analogy is utilized Using their technique, a new formula for the torsional rigidity D_{66} of corrugated board has been calculated [25]

$$D_{66} = \frac{G^l_{12}}{2}(4H^2h + 4Hth + 4Hh^2 + (t^2 + 2th + h^2)h + \frac{h^3}{3}) \qquad (58)$$

SUMMARY AND CONCLUSIONS

In this work, an analytical study on the plate bending stiffnesses of corrugated board has been performed. Formulations to calculate the bending stiffnesses D_{11}, D_{22} D_{12}, and D_{66} of the equivalent plate representing the corrugated board have been established, and then compared to expressions suggested by other investigators. Several methods for modeling the shape of the corrugated orthotropic medium material have been considered including sinusoidal, arc-and-tangent, and elliptical representations. An extension of the membrane analogy method has been used to calculate the torsional rigidity D_{66} of the corrugated board.

ACKNOWLEDGEMENTS

This work was supported by the U.S.D.A. Forest Products Laboratory, Madison, WI, and the Auburn University Pulp and Paper Research and Education Center.

REFERENCES

1. Troitsky, M. S., Stiffened Plates: Bending, Stability and Vibrations, Elsevier Scientific Publishing Company, 1976.
2. Troitsky, M. S., Orthotropic Bridges: Theory and Design, J. F. Lincoln Arc Welding Foundation, 1967.
3. Bares, R. and Massonnet, C., Analysis of Beam Grids and Orthotropic Plates, Frederick Ungar Publishing Company, 1968.
4. Seydel, V. E., "Shear Buckling of Corrugated Plates," (in German), Jahrbuch die Deutschen Versuchsanstalt für Luftfahrt, pp. 233-245, 1931.
5. Lekhnitskii, S. G., Anisotropic Plates, Gordon and Breach Science Publishers, 1968.
6. Szilard, R., Theory and Analysis of Plates, Prentice-Hall, 1964.
7. Kinloch, H. and Harvey, J. M., "Analysis and Design of Anisotropic Plate Structures, with Particular Reference to Decking Systems," in Thin-Walled Structures, Edited by A. H. Chilver, pp. 271-299, Chatto and Windus, 1967.
8. Libove, C. and Hubka, R. E., "Elastic Constants for Corrugated-Core Sandwich Plates," NACA Technical Note 2289, pp. 1-105, NACA, 1951.
9. Blodgett, H. B., "Moment of Inertia of Corrugated Sheets," Civil Engineering, Vol. 4(9), pp. 492-493, 1934.
10. Wolford, D. S., "Sectional Properties of Corrugated Sheets Determined by Formula," Civil Engineering, Vol. 24(2), pp. 59-60, 1954.

11. McKee, R. C., Gander, J. W. and Wachuta, J. R., "Flexural Stiffness of Corrugated Board," Paperboard Package, Vol. 47(12), pp. 111-117, 1962.
12. McKee, R. C., Gander, J. W. and Wachuta, J. R., "Compression Strength Formula for Boxes," Paperboard Package, Vol. 48(8), pp. 149-159, 1963.
13. Kellicutt, K. Q. and Peters, C. C., "Relationship of Moment of Inertia to Stiffness of Corrugated Board," Package Engineering, Vol. 4(8), pp. 84-86, 1959.
14. Kellicutt, K. Q., "How Paperboard Properties Affect Corrugated Container Performance," Tappi, Vol. 44(3), pp. 201A-204A, 1961.
15. Ranger, A. E., "The Compression Strength of Corrugated Fiberboard Cases and Sleeves," Paper Technology, Vol. 1(5), pp. 531-541, 1960.
16. Peterson, W. S., "Minimum Cost Design for Corrugated Containers under Top to Bottom Compression," Tappi, Vol. 63(2), pp. 143-146, 1980.
17. Carlsson, L., Fellers, C. and Jonsson, P., "Bending Stiffness of Corrugated Board under Special Consideration of Asymmetrical and Multiply Construction," (in German), Das Papier, Vol. 39(4), pp. 149-156, 1985.
18. Pommier, J. C., Poustis, J., Fourcade, E. and Morlier, P., "Determination of the Critical Load of a Corrugated Box Subjected to Vertical Compression by Finite Elements Methods," in Proceedings of the 1991 International Paper Physics Conference, pp. 437-447, Kona, HI, 1991.
19. Pommier, J. C. and Poustis, J., "Bending Stiffness of Corrugated Board Prediction Using the Finite Elements Method," in Mechanics of Wood and Paper Materials, Edited by R. W. Perkins, ASME AMD-Vol. 112, pp. 67-70, 1990.
20. Urbanik, T. J., "Effect of Paper Stress-Strain Characteristics on Strength of Singlewall Corrugated Fiberboard," FPL Research Paper #401, U.S.D.A., pp. 1-15, 1981.
21. Peterson, W. S. and Fox, T. S., "Unified Container Performance Theory," in Paper Science and Technology: The Cutting Edge, pp. 172-189, 1979.
22. Peterson, W. S., "Unified Container Performance and Failure Theory-1. Theoretical Development of Mathematical Model," Tappi, Vol. 63(10), pp. 75-79, 1980.
23. Huber, M. T., Theory of Plates, L'vow, 1921.
24. Down, A. G., "The Effect of Flute Profile Changes on Take-Up Ratio and Medium Cost," in the Proceedings of the 1983 Tappi Corrugated Containers Conference, Corrugated Rolls Workshop, pp. 1-9, Chicago, IL, 1983.
25. Luo, S., "Analytical and Experimental Investigation on Corrugated Board," M.S. Thesis, Auburn University, 1991.

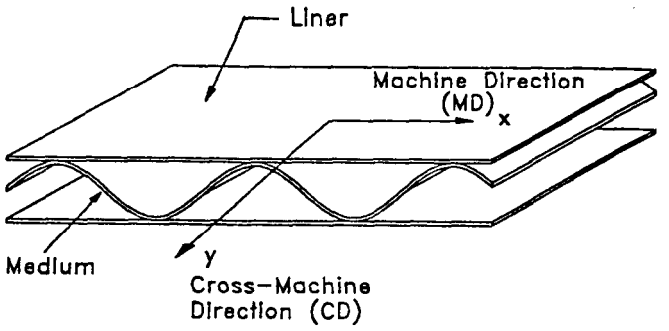

Figure 1- Basic Geometry and Component Materials of Corrugated Board

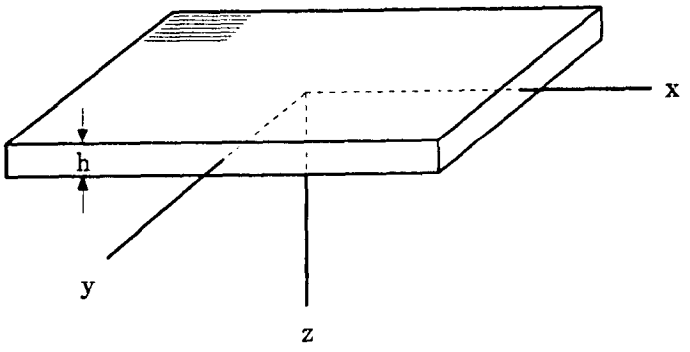

Figure 2 - Thin Orthotropic Plate

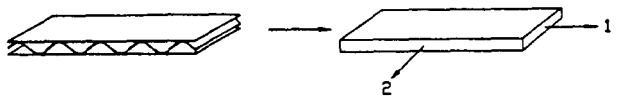

Figure 3 - Orthotropic Equivalent Plate Model for Corrugated Board

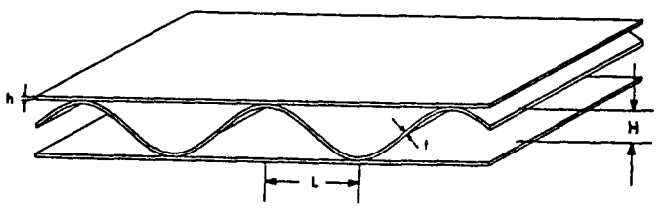

Figure 4 - The Characteristic Geometry and Dimensions of Corrugated Board

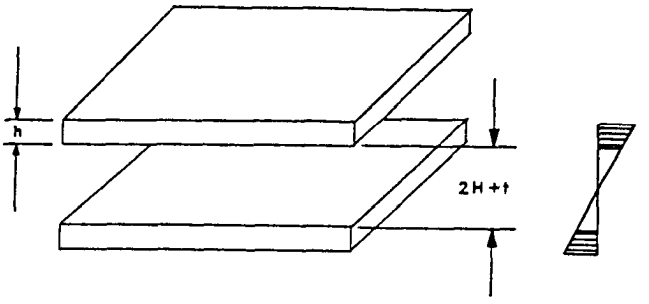

Figure 5 - Geometry of The Liners

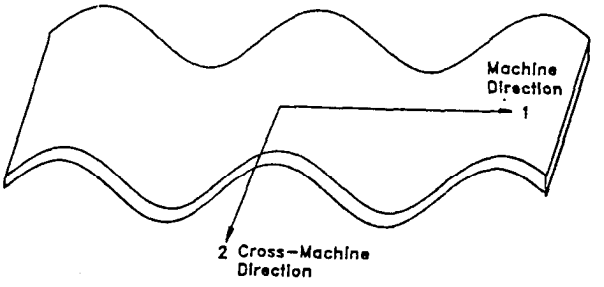

Figure 6 - Principal Material Directions of the Corrugated Orthotropic Medium Material

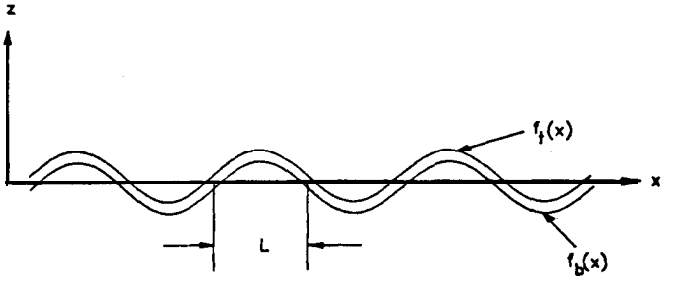

Figure 7 - Top and Bottom Curves Which Enclose the Cross-Sectional Area of the Medium

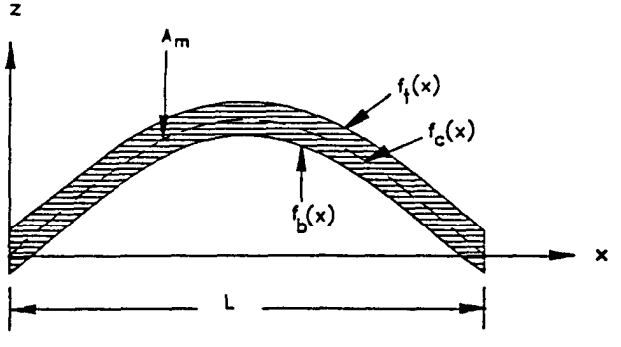

Figure 8 - Area A_m for Evaluation of the Moment of Inertia Per Unit Length of the Medium

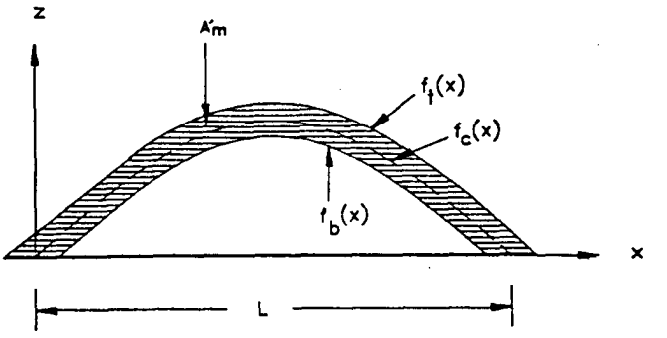

Figure 9 - Area A'_m for Approximate Evaluation of the Moment of Inertia Per Unit Length of the Medium

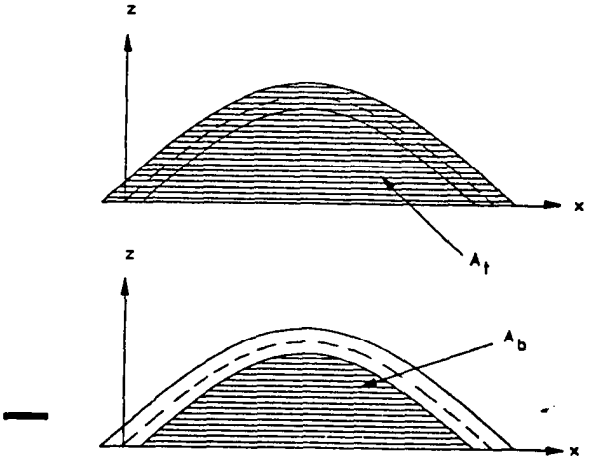

Figure 10 - Area A'_m can be Expressed as the Difference of Area A_t and A_b

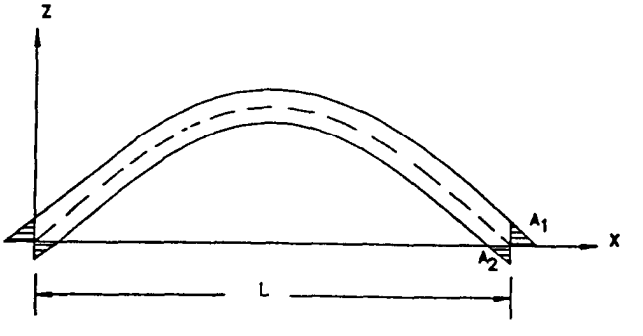

Figure 11 - The Differences between the Areas A_m and A'_m

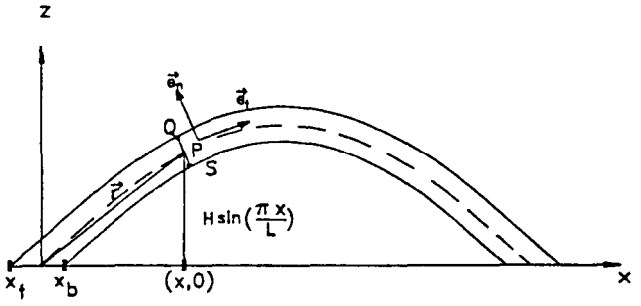

Figure 12 - Sinusoidal Corrugation with Constant Thickness

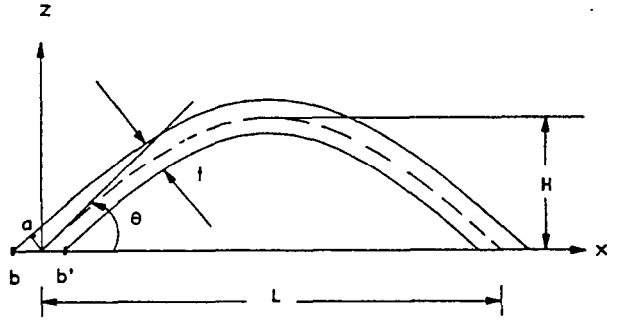

Figure 13 - Geometry and Dimensions for the Sinusoidal Corrugation with Variable Thickness

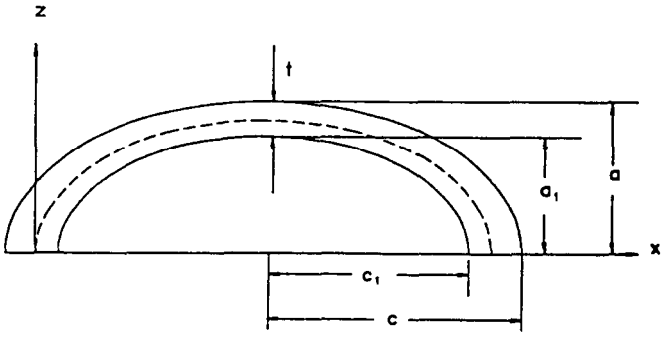

Figure 14 - Geometry and Dimensions for the Semi-Elliptical Corrugation

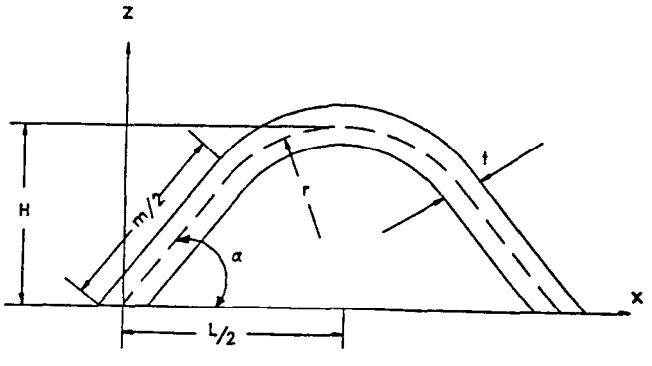

Figure 15 - Geometry and Dimensions for the Arc-and-Tangent Corrugation

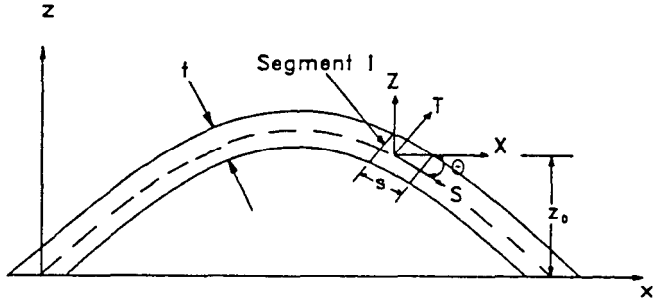

Figure 16 - Geometry and Dimensions for the Line Segments Used in the Ranger-Peterson Method

Type	L (in.)	H (in.)	t (in.)
A Flute	.167	.083	.01
B Flute	.120	.047	.01
C Flute	.143	.071	.01

Figure 17 - Typical Dimensions of Standard Corrugated Mediums

Method of Calculation	A Flute Moment of Inertia Per Unit Length (in^3)	B Flute Moment of Inertia Per Unit Length (in^3)	C Flute Moment of Inertia Per Unit Length (in^3)
Sinusoidal (Constant Thickness)	4.32×10^{-5}	1.40×10^{-5}	3.16×10^{-5}
Sinusoidal (Approximate)	4.09×10^{-5}	1.27×10^{-5}	3.00×10^{-5}
Semi-Elliptical	5.42×10^{-5}	1.66×10^{-5}	3.97×10^{-5}
Arc-and-Tangent	4.26×10^{-5}	1.23×10^{-5}	3.14×10^{-5}
Ranger-Peterson	4.31×10^{-5}	1.29×10^{-5}	3.15×10^{-5}

Figure 18 - Calculations of the Moment of Inertia Per Unit Length for Typical Corrugated Mediums

AMD-Vol. 145
MD-Vol. 36

MECHANICS OF CELLULOSIC MATERIALS

PRESENTED AT
THE WINTER ANNUAL MEETING OF
THE AMERICAN SOCIETY OF MECHANICAL ENGINEERS
ANAHEIM, CALIFORNIA
NOVEMBER 8-13, 1992

SPONSORED BY
THE APPLIED MECHANICS DIVISION AND
THE MATERIALS DIVISION, ASME

EDITED BY
R. W. PERKINS
SYRACUSE UNIVERSITY

THE AMERICAN SOCIETY OF MECHANICAL ENGINEERS
345 East 47th Street ■ United Engineering Center ■ New York, N.Y. 10017